One-dimensional transport code modeling of the limiter-divertor region in tokamaks

J. M. Ogden, D. E. Post, R. V. Jensen, and F. G. P. Seidl

Princeton University, Plasma Physics Laboratory, Princeton, New Jersey 08544 USA

(Received

ABSTRACT

A model of the limiter-divertor scrape-off region has been incorporated into the BALDUR one-dimensional tokamak transport code. Simulations of PDX and ALCATOR have been carried out for ohmic and neutral beam heated cases. In particular, we have studied how the edge conditions and energy loss mechanisms in PDX depend upon plasma density, and compared our results with analytic estimates. The sensitivity of the results to changes in the transport coefficients and scrape-off model is also discussed.

I. INTRODUCTION

Control of impurities is essential in high temperature tokamak experiments and proposed reactor designs. One promising method of impurity control is the magnetic divertor. The divertor reduces impurity influx from the vessel wall to the plasma by channelling the edge plasma into a separate chamber where it is collected by a divertor plate. The divertor action directs incoming impurities away from the main plasma, and lowers the edge temperature of the plasma, which reduces the amount of impurity sputtered at the wall by charge exchange neutrals. In steady state, the plasma loses some of its energy to the divertor plate, and the remainder to the vessel walls by charge exchange, radiation, and a small amount of conduction and convection. Estimates of how much power is lost in each of these ways are important for evaluating how well the system protects the walls and for designing the divertor plates to withstand the necessary heat loads. In order to study the edge conditions and power balance in a tokamak with a divertor, we have incorporated a model of the divertor region in the BALDUR 1-D transport code [1].

We have described the plasma flow to the divertor using the "sheath" model [2]. Assuming that the divertor plate is an insulated conductor, with no net current flow, it is well known that a sheath potential builds up which attracts ions and repels some of the electrons. The flow velocity of

the ions to the plate is approximately the ion sound speed $v_s = [(T_e+T_i)/m_i]^{\frac{1}{2}}$. The predictions of the sheath model are in fair agreement with measurements of the divertor (or limiter) region in PM-1 [3], ALCATOR [4] and DIVA [5].

The usual 1-D transport equations [6] have been modified in the scrape-off region to include particle and energy sink terms representing the losses to the divertor, calculated from the sheath model. The model is self-consistent in that the loss terms depend upon the density and temperature at each time step. We have chosen the transport coefficients in the scrape-off to be approximately the Bohm values, in accordance with experimentally measured diffusion rates, which are roughly the order of Bohm.

The edge conditions in a tokamak are strongly affected by the presence of recycling neutrals. In a tokamak with a divertor or limiter, the energy of the recycling neutrals depends upon the sheath potential near the plate. Typically, the sheath potential is several times kT_{eb}/e, where T_{eb} is the electron edge temperature, depending on the geometry and secondary electron emission at the plate. The ions incident on the plate are accelerated through this potential to an energy considerably higher than the average ion energy just inside the separatrix. Neutrals formed when the accelerated ions impact the plate may have energies of several kT_{eb}. For the limiter case, the neutrals recycle into the plasma where they are ionized or undergo charge exchange or hit the wall. There is experimental

evidence that the average ion energy near the limiter edge in PLT is much larger than the electron temperature at the edge [7]. For the divertor case, recycling near the plate occurs in a chamber remote from the main plasma. The effect of ion acceleration is less obvious than in the limiter case, although it probably increases the edge ion temperature.

The neutral density and energy profiles are determined in the BALDUR transport code by a Monte Carlo method. Neutrals with a given energy distribution are introduced into the plasma at the edge and followed inward. In each radial zone the probability for charge exchange or ionization is computed, yielding the neutral profiles. We have used several different energy distributions for the incoming neutrals in order to study how the edge temperature depends on recycling conditions.

We have used the transport code with divertor or limiter boundary conditions to simulate PDX, ALCATOR, and INTOR. PDX cases with ohmic heating and 6 MW of neutral beam heating were run. The dependence of the edge parameters and power balance on the average plasma density was investigated. A study of how recycling conditions effect the scrape-off was also carried out. Cases were run corresponding to cold recycling from the wall (Franck-Condon neutrals of energy 3 eV), recycling at the limiter edge (neutrals of energy ~ kT_{ib}, where T_{ib} is the edge ion temperature), and ion acceleration (neutrals of energy ~ 2-3 kT_{ib}). Estimates of the incident power density on the divertor plate were made. A comparison with ALCATOR

edge data was done in which the code gave fair agreement within the rather large experimental uncertainty. Simulations of the proposed INTOR experiment were also done.

Simple analytic estimates of edge parameters have been used in the past to design divertor experiments. It is interesting to see how well these estimates agree with the code results. We have compared the usual back of the envelope values with the simulation results. Agreement was typically rather poor, within a factor of 2 - 10, pointing to the fact that a sophisticated treatment of recycling conditions is necessary especially for estimating the ion edge temperature. Finally, we looked at the sensitivity of the numerical results to charges in the main plasma transport model and edge model.

II. MODEL OF THE SCRAPE-OFF REGION

A. The sheath model

We have used the sheath model [2] of the plasma interaction with the divertor or limiter plate. The plate is taken to be an insulated conductor at the edge of the plasma. Since no net current flows to the plate, the fluxes of positive and negative charge must be equal. The limiter plate assumes a negative potential, repelling some of the electrons, so that the electron and ion fluxes balance. (In the absence of this potential buildup, the electron flux $\propto \frac{n \bar{v}_e}{4}$ would exceed the ion flux $\propto \frac{n \bar{v}_i}{4}$ because, $\bar{v}_e$, the electron thermal velocity, is typically much larger than $\bar{v}_i$, the ion thermal velocity.) As is well known from electric probe theory [8], a sheath region forms near a conducting plate held at a fixed potential, which is immersed in a plasma. For an insulated plate, all the ions entering the edge of the sheath are collected at the plate. These ions have approximate flow velocity of $v_s = [(T_e + T_i)/m_i]^{\frac{1}{2}}$. The energy deposited on the plate by the ions and electrons can be calculated by integrating the energy of the particles incident on the limiter plate times the distribution function of these particles in velocity space.

The results for the ion particle flux and the electron and ion energy fluxes to the plate are

$$\Gamma_n = nv_s \tag{1}$$

$$\Gamma_i = 2kT_e\, nv_s \tag{2}$$

$$\Gamma_e = 2kT_e\, nv_s\, \gamma, \tag{3}$$

where γ is a factor, which depends upon secondary electron emission from the plate. For most of our simulations, we have taken $\gamma = 2.9$, which corresponds to no secondary electron emission.

B. The transport equations in the scrape-off

The density and energy diffusion equations in the scrape-off region include loss terms corresponding to particle and energy flows to the divertor or limiter.

Let us approximate the tokamak as a long cylinder of radius a (Fig. 1). For r>a, the system is periodic along the z-axis with period length 2L determined by the geometry of the tokamak. For a tokamak with a toroidal limiter $2L = 2\pi R$, where R is the major radius of the tokamak. For a poloidal divertor $2L = 2\pi R\, q(a)$, since a field line must travel around the torus about q(a) times from the divertor plate before encountering it again. L can be thought of as the average path length of a particle in the scrape-off.

The ion continuity equation is

$$(\partial n/\partial t) + \nabla\cdot(n\vec{v}) = S_n, \qquad (4)$$

where S_n is the ionization source term. The term $\nabla\cdot(n\vec{v})$ can be rewritten $\nabla\cdot(n\vec{v}) = \nabla_\perp\cdot(n\vec{v}_\perp) + \nabla_z\cdot(n\vec{v}_z)$, where $\nabla_\perp\cdot(n\vec{v}_\perp)$ is the radial diffusion term, and $\nabla_z\cdot(n\vec{v}_z)$ is the diffusion along $\hat{z}$-direction (along the field lines) due to the limiter. The limiter acts as a sink for particles, with the particle flux at the limiter plates (at $z = \pm L$) given by Eq. 1. We

approximate $\nabla\cdot(n\vec{v}_2) \simeq \nabla\cdot\Gamma_n$ by $+\Gamma_n/L$ and $\nabla\cdot(n\vec{v}_1)$ by $-\nabla\cdot(D_\perp\nabla n)$. Equation (4) becomes

$$\frac{\partial n}{\partial t} = \nabla\cdot(D_\perp\nabla n) - \frac{nv_s}{L} + S_n \qquad (5)$$

Similarly in the ion and electron energy equations, we make the approximations

$$\nabla\cdot\Gamma_i = \Gamma_i/L \text{ and } \nabla\cdot\Gamma_e = \Gamma_e/L \text{ yielding,}$$

$$\frac{3}{2}\frac{\partial \varepsilon_i}{\partial t} = \nabla\cdot(K_i\nabla T_i - \frac{3}{2}T_iD_\perp\nabla n) - \frac{2\varepsilon_i v_s}{L} + \text{Sources} - \text{Sinks} \qquad (6)$$

$$\frac{3}{2}\frac{\partial \varepsilon_e}{\partial t} = \nabla\cdot(K_e\nabla T_e - \frac{3}{2}T_eD_\perp\nabla n) - \frac{2\gamma\varepsilon_e v_s}{L} + \text{Sources} - \text{Sinks} \qquad (7)$$

where $\varepsilon_i = nT_i$, $\varepsilon_e = nT_e$, $\gamma = 2.9$ (from Eq. 3). Equations (5) - (7) determine the radial transport in scrape-off.

The BALDUR 1-D transport code solves the radial transport equations, and the curl - B Maxwell equation for the poloidal magnetic field. The complete set of equations with details of the numerical methods are documented in Refs. [1] and [6]. We have replaced the usual density and energy diffusion equations with Eqs. (5) - (7). In addition, we have specified the current J_s in the scrape-off layer. Clearly J_s is quite small. J_s can be approximated using the "double probe formula" [4] as

$$J_s = \frac{nev_s}{4}\tanh\left[e\,\phi(z)/2kT_e\right] \leq \frac{nev_s}{4}, \quad r \geq a, \qquad (8)$$

where $\phi(z)$ is the electrostatic potential along the field line near the plate $e\phi(z) \sim 2kT_e$. In the BALDUR transport code, the resistivity η is specified in the solution of the B poloidal equation. We have used an iterative prescription for η, which assures that $J_\parallel < \frac{nev_s}{4}$. This procedure introduces only small errors, since $\frac{nev_s}{4}$ is very small compared to the main plasma current.

C. Neutral model

The edge conditions in a tokamak are affected by the presence of recycling neutral particles from the wall and divertor or limiter. In a tokamak with a limiter or divertor, the sheath potential near the plate may accelerate incident ions, to energies of several kT_e. These ions produce neutrals at the plate which return to the plasma or hit the wall. Neutrals are also generated when ions diffuse into the wall. The energy distribution of the recycled neutrals depends on the edge temperature and the sheath potential. The percentage of lost ions, which return as neutrals, depends upon the recycling coefficient of the walls and divertor.

The Monte Carlo neutral treatment in BALDUR is described in Ref. [9]. A number of neutral particles with a preset energy distribution are launched into the plasma at the edge. Each particle is followed as it moves inward and the probabilities for charge exchange and ionization are computed in each radial zone. Whenever a neutral is ionized, it is added to a source function of ions. If charge exchange occurs the new neutral is

followed, and the change in ion energy is accounted for in the ion energy equation. The neutral is followed until it is ionized or passes completely through the plasma, in which case it is discarded. The resulting ionization source function is normalized so that a percentage of the total number of ions which hit the divertor end walls are returned as ionized particles. The recycling coefficient which determines this percentage is an input parameter to the code.

The energy distribution of incoming neutrals is also set as input to BALDUR. In order to study how sensitive edge conditions are to the recycling neutrals, we have carried out runs with several models. In the first model, we have assumed that all the recycled neutrals both from the wall and the divertor or limiter are cold with Franck-Condon dissociation energy of 3 eV. The second model returns neutrals to the plasma with an energy spread equal to the ion temperature at the limiter edge. In the third model, we assume that the ions are accelerated by the sheath potential near the plate and return them with an energy of $2\text{-}3kT_e$.

The presence of neutrals in the scrape-off has another effect on the plasma interaction with the limiter, namely "neutral friction." When the ions flowing to the limiter encounter neutrals, charge-exchange occurs with a probability determined by the local density and temperature. The effect of the charge-exchange is to replace the plasma ion with a less energetic ion, reducing the ion flow rate to the limiter. This

flow rate in steady state can be computed from the momentum equation for ions parallel to the field.

The scrape-off loss terms in Eqs. (5)-(7) become

$$\frac{nv_s}{L} \Rightarrow \frac{v_s n}{L} \quad \frac{1}{1 + \frac{L\nu_c}{4 v_s}} \tag{9}$$

$$\frac{2\varepsilon_e v_s \gamma}{L} \Rightarrow \frac{2\varepsilon_e v_s}{L}\gamma \quad \frac{1}{1 + \frac{L\nu_c}{4 v_s}} \tag{10}$$

$$\frac{2\varepsilon_i v_s}{L} \Rightarrow \frac{2 v_s \varepsilon_i}{L} \quad \frac{1}{1 + \frac{L\nu_c}{4 v_s}} , \tag{11}$$

where $\nu_c = n_o \langle \sigma_{cx} v \rangle$ is the charge-exchange frequency. These modified scrape-off loss terms are used in most of our simulations.

D. Transport model in the scrape-off

The transport coefficients in the scrape-off layer have not been determined from experiment. Recent DIVA results [5] show a density diffusion rate equal to about 10% of the Bohm value; DITE results indicate diffusion several times Bohm. We have used transport coefficients in the scrape-off region equal to a constant of order one times the Bohm coefficients for most of our runs. In the main plasma, the density diffusion coefficient $D_\perp$ and the electron heat conductivity K_e have been chosen empirically

to give the best fit to existing data or expected parameters. For most runs $D_\perp$ and K_e are proportional to $1/n_e$. The Ware pinch effect is included in K_e and $D_\perp$. The neoclassical value for the ion heat conductivity K_i has been used.

E. Estimates of edge parameters

The parameters in the scrape-off region can be estimated in steady state from the transport Eqs. (5) - (7). The estimates given below have been used in the design of divertor experiments, and it is interesting to see how well they match the numerical results. We assume slab geometry near the separatrix, and the radial coordinate is replaced by x.

Let us assume that the density and temperatures near the separatrix (x=a) have radial dependence of the form

$$n(x) = n(a)e^{-(x-a)/\lambda_n} \tag{12}$$

$$T_e(x) = T_e(a)e^{-(x-a)/\lambda_T} \tag{13}$$

$$T_i(x) = T_i(a)e^{-(x-a)/\lambda_i} \quad . \tag{14}$$

In steady state, the time derivatives in the transport equation go to zero. The density diffusion equation becomes

$$0 = \frac{\partial}{\partial x}\left(D\,\frac{\partial n}{\partial x}\right) - \frac{nv_s}{L} + S_n \quad , \tag{15}$$

where S_n is a density source term due to ionization of neutrals. The electron energy equation is

$$0 = \frac{\partial}{\partial x}\left(K_e\,\frac{\partial T_e}{\partial x} + \frac{3}{2}T_e D\,\frac{\partial n}{\partial x}\right) - \frac{2\gamma n T_e v_s}{L} + \text{Sources} - \text{Sinks} \tag{16}$$

where the source terms are ohmic and beam heating, and sink terms are radiation, ionization and temperature equilibration losses. The ion energy equation is

$$0 = \frac{\partial}{\partial x}\left(K_i \frac{dT_i}{\partial x} + \frac{3}{2}T_i D \frac{\partial n}{\partial x}\right) - \frac{2nT_e V_s}{L} + \text{Sources-Sinks}, \tag{17}$$

where source terms are from beam heating and temperature equilibration, and the main sink term is charge exchange.

We wish to find expressions for λn, λ_T, λ_i, $n(a)$, $T_e(a)$ and $T_i(a)$ in terms of the main plasma parameters. Define particle and energy confinement times as the total number of particles or energy divided by the losses. The particle confinement time τ_p is

$$\tau_p \equiv \frac{\bar{n} \cdot V}{D \frac{\partial n}{\partial x}\Big|_{x=a} \cdot A} \tag{18}$$

where V is the plasma volume inside the separatrix and A is its surface area, $\bar{n}$ is the volume averaged density and $D\ \partial n/\partial x$ is the particle flux across the separatrix. The electron energy confinement time τ_{eE} is

$$\tau_{eE} \equiv \frac{\overline{\frac{3}{2}nT_e} \cdot V}{\left(K_e \frac{\partial T_e}{\partial x} + \frac{3}{2}T_e D \frac{\partial n}{\partial x}\right) \cdot A + (\bar{W}_{Rad} + \bar{W}_{ion}) \cdot V} \tag{19}$$

where $\overline{W_{Rad}}$ and $\overline{W_{ion}}$ are volume averaged radiation and ionization losses from the main plasma and $K_e\ \partial T_e/\partial x + \frac{3}{2} T_e D\ \partial n/\partial x$ electron energy is the flux across the separatrix due to conduction and convection. Similarly, the ion energy confinement time τ_{iE} is given by

$$\tau_{iE} = \frac{\frac{3}{2}\,\overline{n\,T_i}\cdot V}{\left(K_i \frac{\partial T_i}{\partial x} + \frac{3}{2} T_i D \frac{\partial n}{\partial x}\right)\cdot A + \bar{W}_{cx}\cdot V} \qquad (20)$$

where $\bar{W}_{cx}$ is the volume averaged charge exchange loss.

1. Edge density and density scrape-off width

Let us substitute the form of Eq. (12) for the density into Eq. (15). At r = a, we find

$$0 = D(a)\frac{n(a)}{\lambda_n^2} - n(a)\,\frac{v_s}{L} + S_n(a). \qquad (21)$$

The ionization source function may be written as

$$S_n(a) = n(a)n_o(a)\langle\sigma v\rangle_i = n(a)/\tau_i, \qquad (22)$$

where τ_i is the average time it takes to ionize a particle at x = a. Defining the average time a particle spends in the scrape-off $\tau_{||} \equiv v_s/L$, Eq. (21) becomes

$$0 = \frac{D(a)n(a)}{\lambda_n^2} - \frac{n(a)}{\tau_i} + \frac{n(a)}{\tau_{||}}$$

Solving for the density scrape-off width,

$$\lambda_n = \left[D(a)\left(\frac{\tau_i\ \tau_{||}}{\tau_i - \tau_{||}}\right)\right]^{1/2} \qquad (23)$$

Note that if the ionization source function $S_n = n(a)/\tau_i$ balances the loss to the divertor $n(a)/\tau_{||}$, e.g. $\tau_i = \tau_{||}$, the density profile is flat, with $\lambda_n \to \infty$.

If the particle confinement time is known, the edge

density may be found in terms of the main plasma parameters from Eq. (18).

$$\tau_p = \frac{\bar{n} \cdot \pi a^2 \; 2\pi R}{D\frac{n(a)}{\lambda_n} \cdot 2\pi a \; 2\pi R} = \frac{\bar{n} \; \lambda_n a}{D \; 2n(a)}$$

or

$$n(a) = \frac{\bar{n}}{2\tau_p} \frac{\lambda_n a}{D} = \bar{n} \frac{a}{2\lambda_n} \frac{\tau_{||}}{\tau_p} \frac{1}{1-\frac{\tau_{||}}{\tau_i}} . \qquad (24)$$

For typical values of scrape-off parameters $\tau_i >> \tau_{||}$ and $n(a) \simeq \bar{n}/20$ and $\lambda_n \simeq 1\text{-}3$ cm.

2. Edge electron temperature and scrape-off width

Similarly, if we substitute the exponential form for $T_e(x)$, Eq. (24) into Eq. (7), we find an expression for λ_T.

$$0 = \frac{K_e(a)T_e(a)}{\lambda_T^2} + \frac{3}{2} T_e(a) \; D(a) \; \frac{n(a)}{\lambda_n} \left(\frac{1}{\lambda_n} + \frac{1}{\lambda_T}\right)$$

$$\frac{-2\gamma n(a) \; T_e(a)}{\tau_{||}} + \text{Sources-Sinks} . \qquad (25)$$

Evaluating the source and sink terms in Eq. (25) shows that only convection and conduction are of the same order as divertor loss for estimated typical scrape-off parameters. Therefore, we ignore the other sources and sinks, yielding a quadratic equation for λ_T in terms of λ_n. Assuming that $K_e(a) \simeq \frac{3}{2}n(a)D(a)$, for Bohm transport, we obtain

$$\lambda_T \simeq 0.7 \quad \lambda_n \qquad (26)$$

for no secondary electron emission, $\gamma = 2.9$. The edge temperature is found in terms of the electron energy confinement time. Since the other energy sources and sinks in Eq. (6) are negligible in the scrape-off, the electron energy flux term $(K_e \partial T_e/\partial x + \frac{3}{2} T_e D \partial n/\partial x) \cdot 2\pi a\, 2\pi R$ is equivalent to energy loss to the divertor $(2\gamma n_e T_e/\tau_{||}) \cdot 2\pi R\, 2\pi a\, \lambda_E$, where λ_E is the energy scrape-off width $\lambda_E = \frac{\lambda n\, \lambda T}{\lambda_T + \lambda_n} \simeq 0.4\, \lambda_n$. Equation (19) for τ_{eE} may be written

$$\tau_{eE} = \frac{\overline{\frac{3}{2} nT_e} \cdot V}{\frac{2\gamma n T_e(a)}{\tau_{||}} \cdot 2\pi R\, 2\pi a \lambda_E + (\overline{W_{rad}} + \overline{W_{ion}}) \cdot V} \qquad (27)$$

or, solving for $T_e(a)$

$$T_e(a) = \frac{3}{4\gamma} \frac{\overline{nT_e}}{n(a)} (1-f) \frac{\tau_{||}}{\tau_{eE}} \frac{a}{2\lambda_E}$$

or, using Eq. (24) with $\tau_i >> \tau_{||}$,

$$T_e(a) \simeq \frac{3}{4\gamma} \bar{T}_e (1-f) \frac{\tau_p}{\tau_{eE}} \qquad (28)$$

Where f is the fraction of the electron energy lost via radiation and ionization in one electron energy confinement time, and 1-f is the fraction lost to the divertor.

3. Edge ion temperature and scrape-off width

Estimates of the ion temperature at the edge require a knowledge of recycling conditions. It is difficult to make simple estimates with confidence. The same sort of analysis as given

above for the electrons yields a scrape-off width for the ion temperature on the order of that for the electrons. The ion edge temperature is approximately

$$T_i(a) = \frac{3}{4} \frac{\tau_p}{\tau_{Ei}} \bar{T}_i \ (1-g) \tag{29}$$

where g is the fraction of the total ion energy lost via charge exchange in one ion energy confinement time, and 1-g is the fraction lost to the divertor.

4. Maximum power density deposited on the divertor plate

The power density deposited on the plate is given by

$$P = 2n(a) \ [T_i(a) + \gamma \ T_e(a)] \ v_s \tag{30}$$

Substituting the expressions for $n(a)$, $T_i(a)$, and $T_e(a)$, we find that

$$P \simeq \alpha \frac{L}{\lambda_n} \frac{W_{in}}{A} \tag{31}$$

where W_{in} is the total input power, ohmic plus beam, A is the plasma surface area, and α is the fraction of the total power loss which goes to the divertor.

III. NUMERICAL RESULTS

A. Steady state results

We have done simulations of PDX and ALCATOR for ohmic and neutral beam heated discharges. In particular, we have studied how the edge parameters and power loss mechanisms depend upon plasma density, for different recycling conditions and transport models.

Typical steady state density and temperature profiles for PDX with 6 MW of neutral beam injection are shown in Figs. 2 and 3. The density and temperatures decrease sharply near the separatrix. A close-up view of the profiles in the scrape-off region is given in Fig. 4. The density and temperatures fall off logarithmically near the separatrix as in Eqs. (12)-(14), with scrape-off width of about 2.5 cm. In Fig. 5 we have sketched how the edge density and temperatures and central plasma temperatures depend on volume averaged plasma density for PDX with 6 MW of neutral D beams into a D^+ plasma. We have assumed that the neutrals recycle with 3 eV energy. As expected from simple estimates, the edge density scales almost linearly with average density, and the edge electron temperature decreases with the central plasma electron temperature. However, the edge ion temperature is held to a fairly low value by the cold recycling neutrals. We shall see that the edge parameters are quite sensitive to the recycling energy. Figure 6 shows the power balance in steady state for PDX with 6 MW neutral beams. The absorbed beam power and ohmic heating power sources are shown

as solid lines. Power loss terms to the divertor, and to the walls via charge exchange and radiation are plotted as dashed lines. Sixty to seventy-five percent of the input power is lost to the divertor. Charge exchange losses are important at lower densities, accounting for ~ 30% of the energy loss at $\langle n \rangle = 1.5 \times 10^{13}$. At higher densities radiation is comparable to charge exchange. Radiation and charge exchange are each responsible for ~15% of the absorbed energy at $\langle n \rangle = 3 \times 10^{14}$. The code ignores beam particles which are not absorbed by the plasma, although in practice this could be an important load on the walls. The peak power density incident on the divertor plate is graphed as a function of $\langle n \rangle$ in Fig. 7. The maximum power density for Ohmically heated cases is shown for comparison. Typically several kilowatts /cm^2 must be dissipated at the divertor plate for the beam cases, and about half a kilowatt/cm^2 for the Ohmically heated cases.

B. Effect of neutral recycling model

As mentioned above, the edge conditions are sensitive to the neutral recycling model. We have studied the effect of recycling neutral energy on PDX with 6 MW of neutral beam heating. Figures 8 and 9 show the edge parameters and power balance vs. $\langle n \rangle$, when the recycling neutral energy is 70 eV. These graphs are analogous to Figs. 5 and 6, (3 eV neutral cases). Not surprisingly, the more energetic 70 eV neutrals penetrate further into the plasma. Fewer neutrals are ionized in the scrape-off and the edge density is lower in the 70 eV case than the 3 eV case. The edge temperatures are higher for higher neutral

recycling energy, but the maximum power loading on the divertor actually decreases, because of the lowered edge density. Comparing the power balance graphs Figs. 6 and 9, we find that charge exchange losses are greater for higher energy neutrals. These losses account for the lower central ion temperature. Figures 10 and 11 illustrate similar results for 300 eV neutrals, corresponding to ion acceleration through the electrostatic sheath near the divertor plate. Table I is a summary of the effect of increasing the neutral recycling energy. Clearly, a wide range of conditions are possible, depending on the recycling neutral energy.

C. Sensitivity of the results

The transport coefficients and flow model in the scrape-off are not known experimentally. We have investigated the sensitivity of our results to changes in the transport coefficients and in the model for the scrape-off loss terms. These studies are based upon trying to match an experimental ALCATOR case with B_z = 55 kG, J = 270 kA, line average density $\bar{n} = 3.5 \times 10^{14}$ cm^{-3} and $T_e(o) \simeq T_i(o) \simeq 800$ eV. The density and temperatures at the limiter radius were measured to be $n_e = 5 \times 10^{13}$, $T_e \simeq 10$ eV, and with a fall-off width λ_n (for the density) of about 1 cm.

1. Changes in the particle flow in the scrape-off

a. Charge exchange friction

The effect of charge exchange between ions and neutrals

in the scrape-off is to reduce the particle flux Γ_n to the divertor limiter increasing $\tau_{||} = n/\Gamma_n$. From Eqs. 9 and 24, we expect that n(a) will increase by a factor $(1 + L\nu_c/4v_s)1/2$, if charge exchange effects are included. Comparing two cases without charge exchange effects $\nu_c = 0$, and with $L\nu_c/4v_s = 1.3$, we find that n(a) increases by a factor of ~ 1.6 with charge exchange. This agrees with the rough estimate, which predicts an increase by a factor of $(2.3)^{1/2}$. The separatrix temperatures are unaffected by the addition of charge exchange, as expected. The scrape-off width increased slightly from 1 cm to 1.2 cm.

b. Average path length in the scrape-off, L

Changes in the average path length in the scrape-off region affect the particle flow rate and therefore the separatrix density. In agreement with rough estimates, n(a) increased as $(L)^{1/2}$, λ_n, $T_e(a)$ and $T_i(a)$ were unchanged by variations in L.

2. Changes in main plasma transport coefficients

a. $D_\perp$

When $D_\perp$ was increased by a factor of 3, the density profile flattened and n(a) increased by a factor of ~ 3. T_e decreased by a factor of ~ 2, and T_i and λ_n were insensitive to changes in $D_\perp$.

b. K_e

When K_e was increased by a factor of 3, $T_e(a)$ increased by a factor of ~ 2. n(a), $T_i(a)$, and λ_n were unchanged.

c. K_i

K_i was taken to be the neoclassical value and was not varied separately.

3. Changes in the scrape-off transport coefficients

Measurements of the diffusion coefficient in the scrape-off have yielded values in the range of 10% of Bohm to several times Bohm. We found very little difference in our results when $D_\perp$, K_e, and K_i in the scrape-off were varied between 0.1 and 10.0 times the Bohm values. The scrape-off width, which one would estimate to depend on $D_\perp^{1/2}$, is essentially unchanged.

D. Comparison of analytic estimates and numerical results

It is interesting to compare the analytic estimates of Section II.E for the edge parameters with the code results. In Table II, we have listed the numerical and analytic values for several PDX cases. The analytic values are conservative in that they consistently predict higher edge temperatures, smaller scrape-off widths, and greater power loading than the simulations. The back of the envelope formulas fare well as cautious design criteria. In most cases, the agreement is rather poor, to within a factor of 2 - 10. The lack of agreement seems to stem from the fact that neutral recycling has the effect of building up the edge density, increasing the scrape-off width, and cooling the edge temperatures. Recycling is included in the code, but not in the analytic estimates.

VI. SUMMARY

We have added a simple model of the limiter, divertor scrape-off region to BALDUR 1-D tokamak transport code. Simulations were done to study how well the divertor protects the system. We calculated the edge density and temperatures and the power load on the vessel walls due to charge exchange and radiation and, the limiter or divertor plate, for ohmically and neutral beam heated cases in PDX and ALCATOR. Ten to thirty percent of the input beam energy is lost immediately by charge exchange or just passes through the plasma. Of the absorbed beam energy, about sixty to eighty percent goes to the divertor, the rest to charge exchange, which dominates at lower densities, and radiation, which becomes comparable to charge exchange or higher densities. For example, of a total of 6.2 MW of input power 6 MW beams plus ohmic power, about 1 MW of beam power is lost immediately, 3.4 MW go to the divertor, 1.6 MW are lost via charge exchange and 0.2 MW via radiation for PDX with $\langle n \rangle = 5 \times 10^{13} cm^{-3}$. Charge exchange losses to the vessel walls are about 10 watts/cm^2. The damage caused at the wall depends upon the energy of the outgoing neutrals. The divertor plate must withstand a maximum loading near, the separatrix of several kilowatts/cm^2. This assumes that the plate is perpendicular to the flow. The power density can probably be decreased by spreading the field lines or tilting the plate.

The edge conditions in tokamaks are not well known experimentally. We tried to estimate how sensitive our results were to changes in these unknown quantities in the model. Changes in the model for the plasma flow to the divertor gave small, predictable changes in the edge values. Changes in the transport coefficients near the edge made essentially no difference in the results. However, the results were very sensitive to the neutral recycling model. If we assumed that the neutrals recycled at 3 eV, the edge temperature was typically rather low (~50 eV) and the central temperature was high. For energetic recycled neutrals, corresponding to acceleration of ions through the electrostatic sheath potential near the plate, the edge temperatures rose and the central temperature decreased. For a typical PDX case with $\langle n \rangle = 3 \times 10^{13}$ and 6 MW of neutral beams, a decrease in $T_i(0)$ from 6.5 keV to 4.5 keV was seen when the recycling neutral energy was raised from 3 eV to 300 eV. The decrease in central temperature resulted from increased charge exchange losses near the plasma center. The 300 eV neutrals penetrated further into the plasma than the 3 eV neutrals, and more energy was lost when they charge exchanged with plasma ions. Clearly, recycling conditions are very important in determining both the edge and main plasma characteristics.

A comparison was made between the typical simple analytic estimates of edge values, and the code results. The estimates were conservative, giving consistently worse edge conditions (higher temperatures, more power loading on the

divertor, smaller scrape-off width) than the code. It appears the recycling neutrals which are included in the code, but not in the analytic estimates, improve the edge conditions by cooling the temperature and widening the scrape-off. The simple analytic estimates give more extreme conditions by a factor of 2 - 10 than the simulations. The estimates are useful as "worst case" design criteria, but are probably unduly pessimistic.

Our code can be used as a basis of comparison for forthcoming results on the current generation of tokamaks with divertor. The numerical results show that recycling conditions of the edge have a large effect on the plasma produced. It is likely that sophicated edge models including impurity species will be needed to understand the experimental results. Judging from the power loads we have predicted, it appears that impurities will be generated at the wall and at the divertor plate. A good model of how the impurities behave near the edge is neccessary to extend our work.

ACKNOWLEDGMENTS

We would like to thank Alan Boozer, Dale Meade, Cliff Singer, and Fred Tenney for helpful discussions.

This work was supported by the US Department of Energy Contract No. EY-76-C-02-3073.

Table 1. Effect of Recycled Neutral Energy on Edge Conditions in PDX with 6 MW Beams

E_0 (eV)	$\bar{n}$ (cm^{-3})	$T_i(0)$ (keV)	$T_e(0)$ (keV)	$n_e(a)$ (cm^{-3})	$T_i(a)$ (eV)	$T_e(a)$ (eV)	λ_n (cm)	P_{max} (kw/cm^2)
3	10^{14}	3.2	3.2	9×10^{12}	50	110	4	3.5
	3×10^{13}	6.5	3.8	1.5×10^{12}	35	180	4	2.0
70	10^{14}	2.8	2.8	1.7×10^{12}	150	200	3	2.2
	3×10^{13}	5.1	3.5	6×10^{11}	130	320	4.5	1.5
300	10^{14}	2.2	2.2	6.5×10^{11}	320	280	2	2.9
	3×10^{13}	4.5	3.3	3×10^{11}	350	420	6	1.4

Table II. Comparison of Edge Values From Analytic Estimate and Simulation for PDX With 6 MW Beams

$\langle n \rangle$ (cm^{-3})	Recycled Neutral Energy (eV)	λ_n (cm)	$n(a)$ (cm^{-3})	$T_e(a)$ (eV)	$T_i(a)$ (eV)	Maximum Power Density (kW/cm^2)	
2.8×10^{13}	3	4	2.2×10^{12}	210	37	1.7	Code
		2	2.8×10^{11}	476	1400	5.9	Est.
1.56×10^{14}	3	4	1.6×10^{13}	82	67	4.3	
		2.8	1.5×10^{12}	320	630	8.0	
4×10^{13}	70	4.5	7.28×10^{11}	361	154	1.6	
		2.2	4×10^{11}	554	1190	5.2	
9×10^{13}	70	3	1.47×10^{12}	255	161	2.1	
		2.2	9×10^{11}	464	903	7.2	
3.8×10^{13}	300	6.5	3.5×10^{11}	477	371	1.6	
		2.6	4×10^{10}	683	749	7.0	
1.20×10^{14}	300	2	2.57×10^{12}	173	286	3.5	
		2.2	1.3×10^{11}	440	670	7.7	

REFERENCES

[1] MCKENNEY, A., et al., BALDUR 1-D Tokamak Transport Code Manual, PPPL, (1978).

[2] HOBBS, G. D., WESSON, J. A., Plasma Phys. 9, (1967), 85.

[3] SCHMIDT, J. A., PPPL, MATT-0-31, (1974).

[4] SCATURRO, L., private communication.

[5] DIVA Group, Nucl. Fusion 18, (1978), 1619.

[6] DÜCHS, D. F., POST, D. E., and RUTHERFORD, P. H., Nucl. Fusion 17, (1977), 565.

[7] COHEN, S. A., et al., submitted to Phys. Rev. Lett.

[8] CHEN, F. F., "Electric Probes," Plasma Diagnostic Techniques, Academic Press, New York, NY, 1965.

[9] HUGHES, M. H., POST, D. E., J. Comput. Phys. 28, (1978), 43.

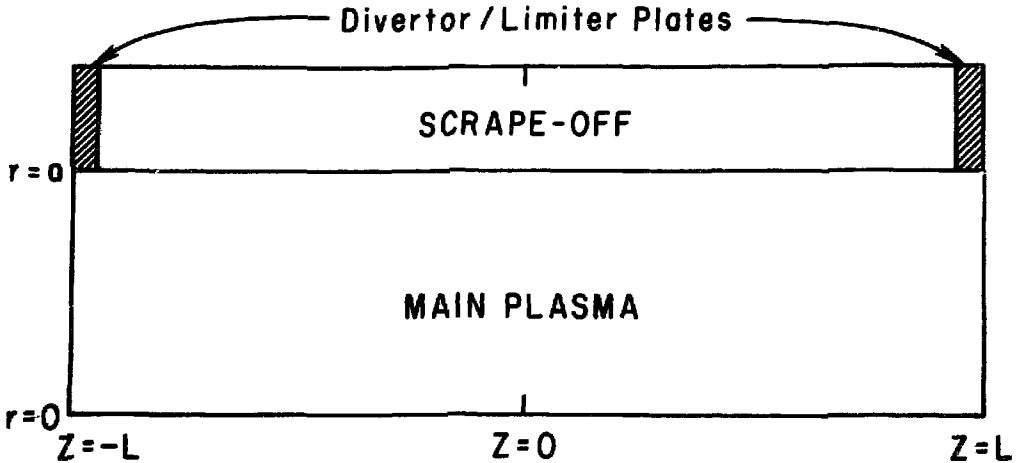

792481

Fig. 1. Geometry of scrape-off region and main plasma in 1-D radial transport code.

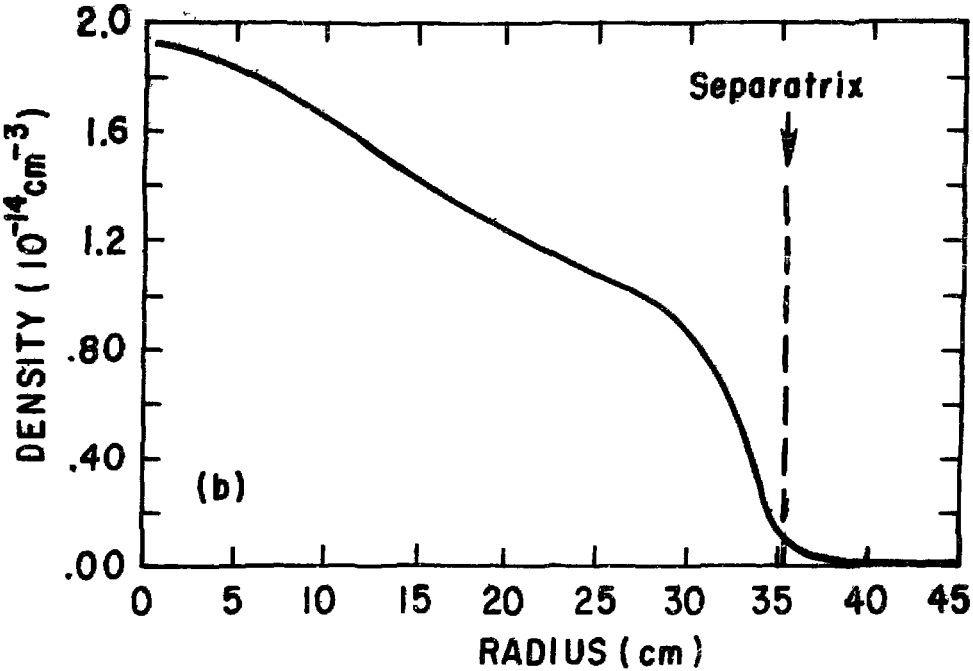

792491

Fig. 2. Steady state density profile - PDX

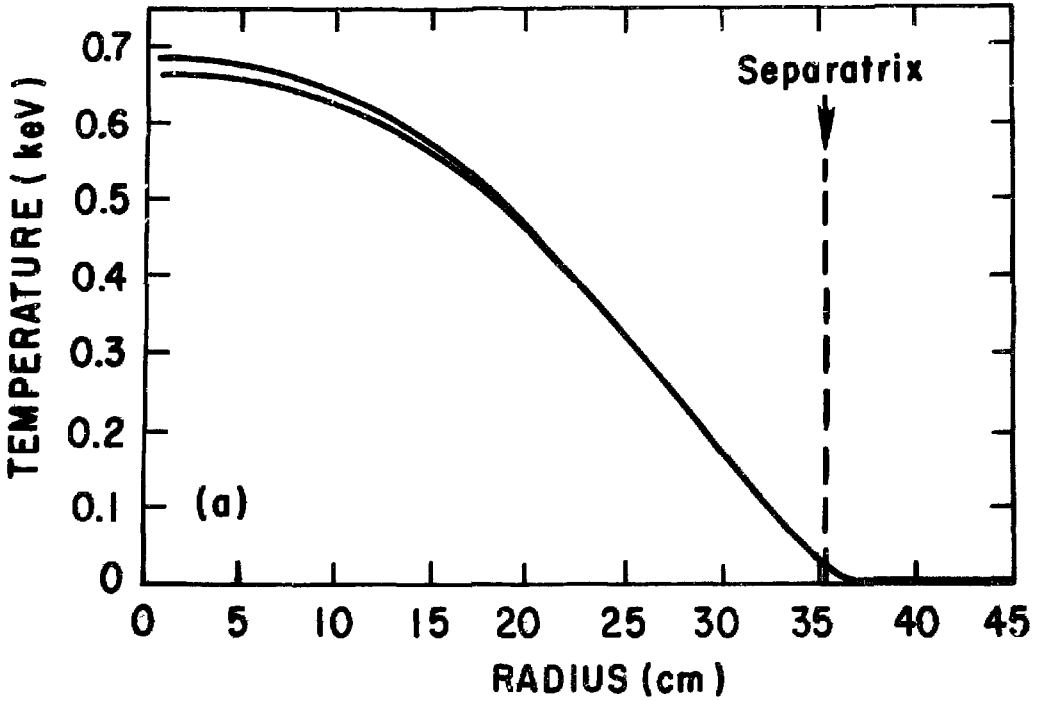

792490

Fig. 3. Steady state temperature profile - PDX.

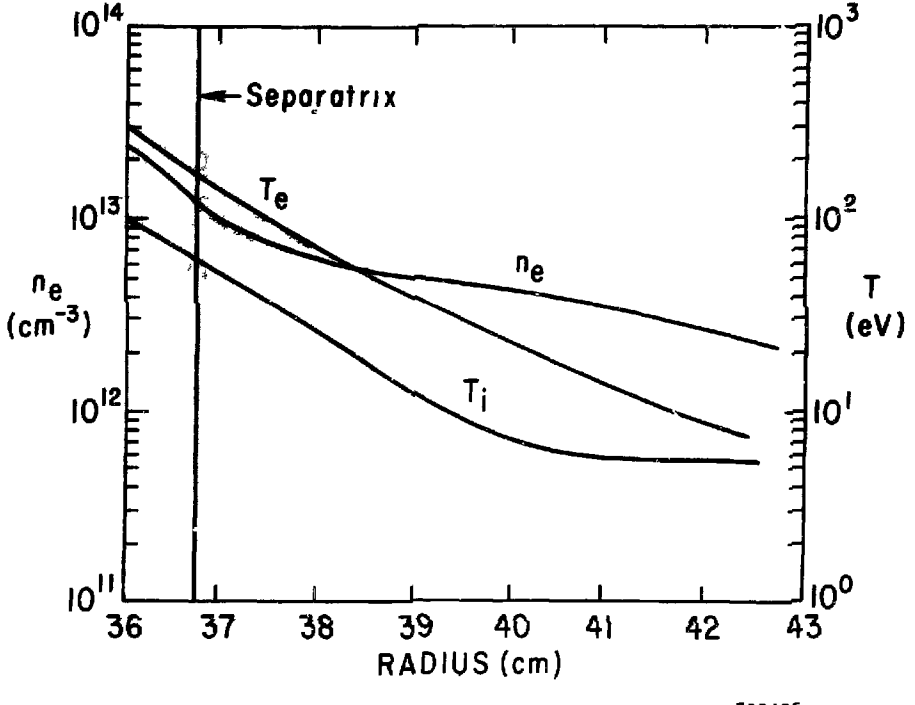

Fig. 4. Scrape-off region, log n, log T_e, log T_i vs radius - PDX.

732486

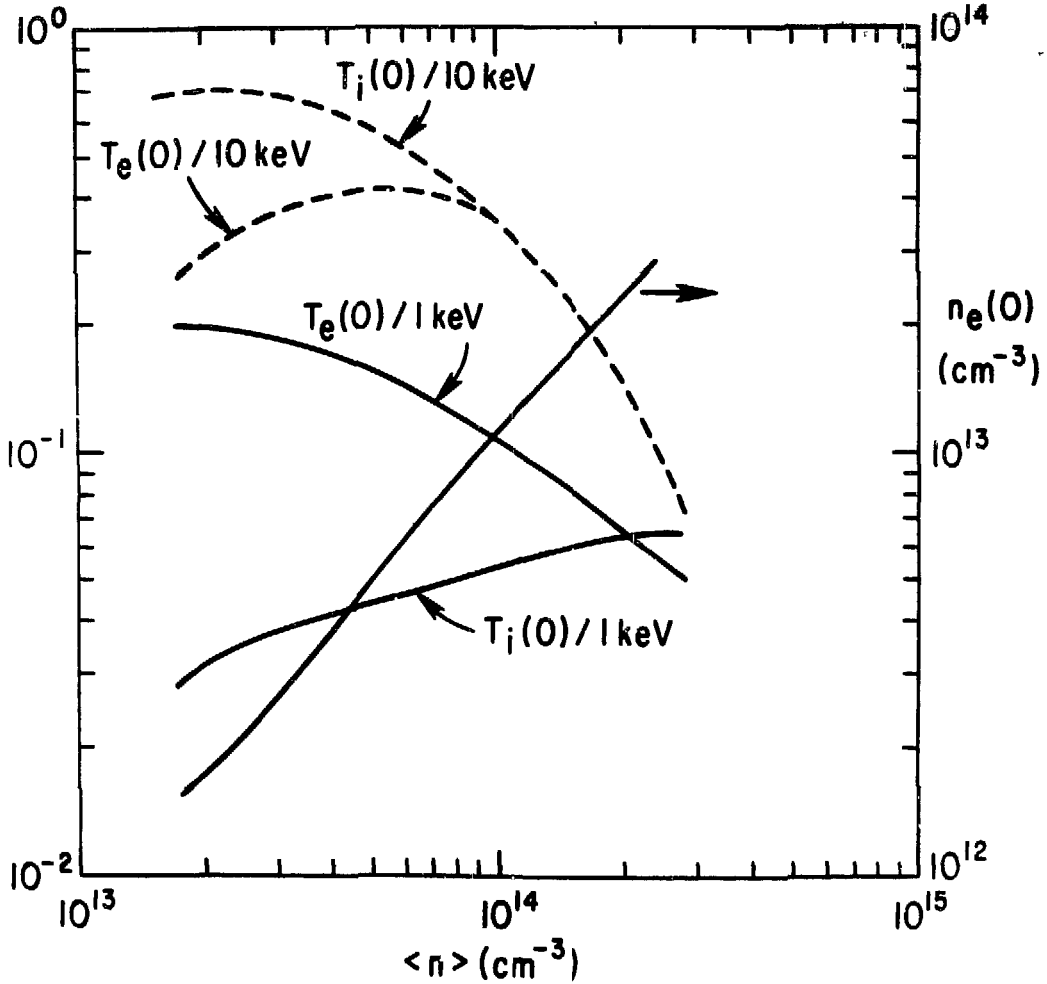

792482

Fig. 5. Edge density and temperatures; central temperatures vs volume averaged density for PDX w/6 MW neutral beams, 3 eV recycled neutrals.

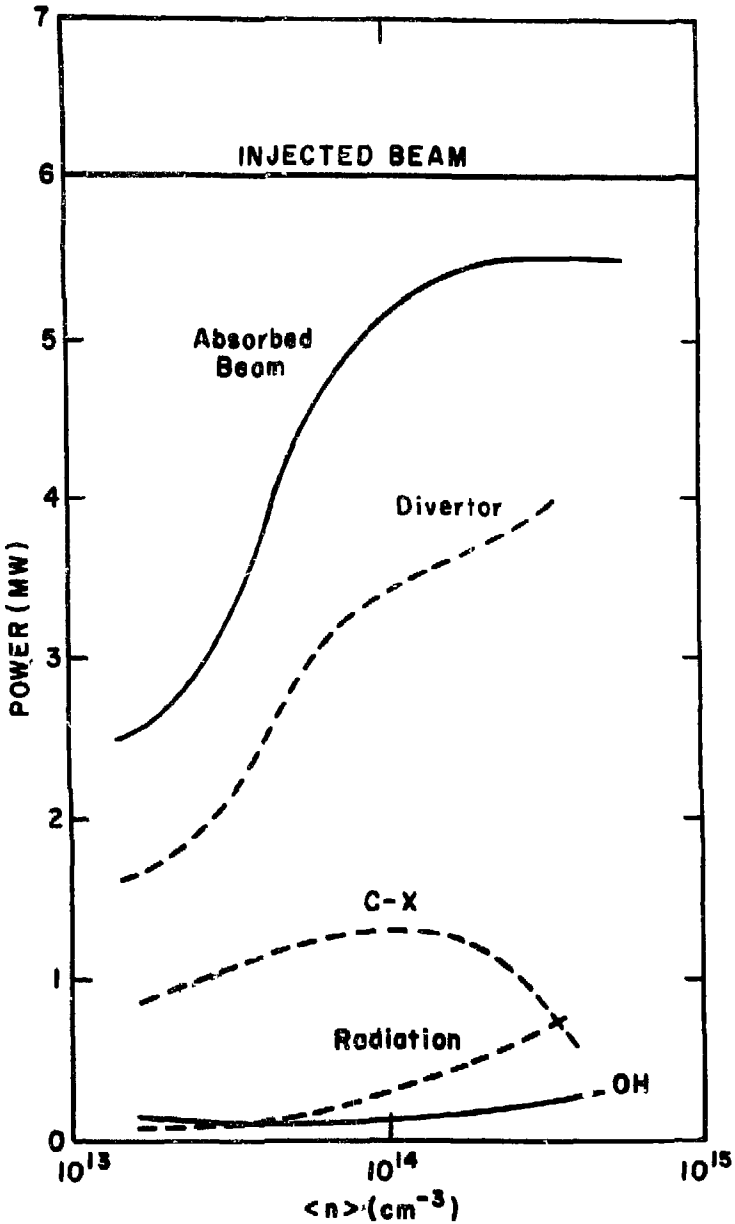

Fig. f. Power balance vs <n> - PDX w/6 MW beams, 3 eV neutrals.

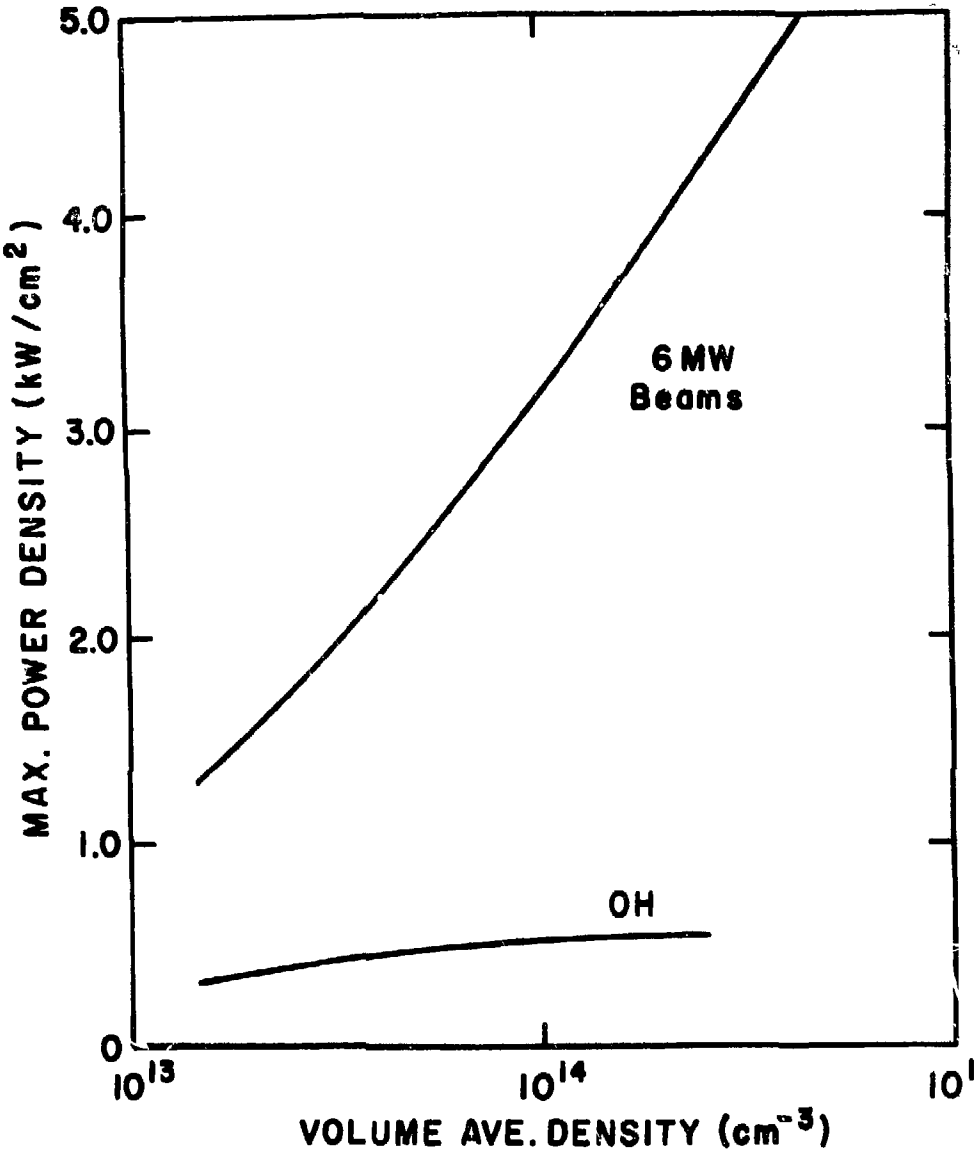

792483

Fig. 7. Maximum power loading on divertor plate vs <n> for PDX with ohmic heating and 6 MW neutral beams.

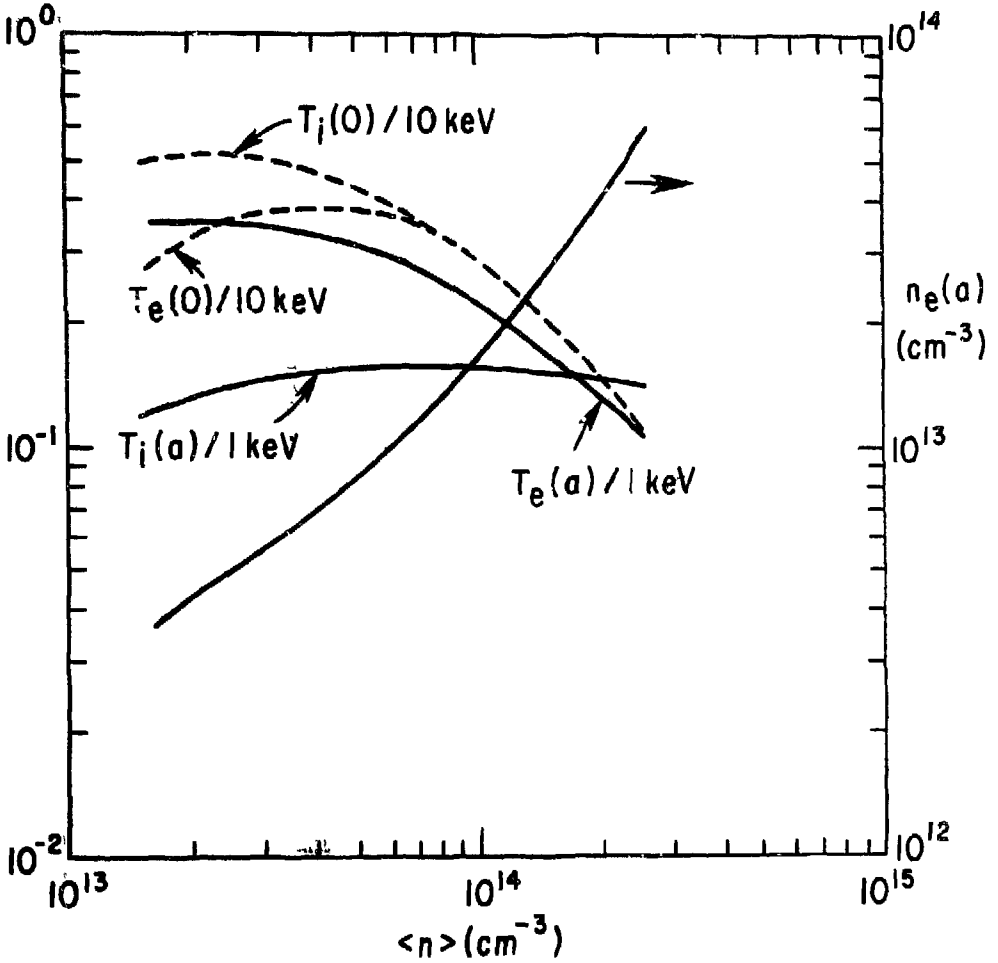

792484

Fig. 8. Edge parameters, central temperatures vs <n> - PDX with 6 MW beams, 70 eV recycled neutrals.

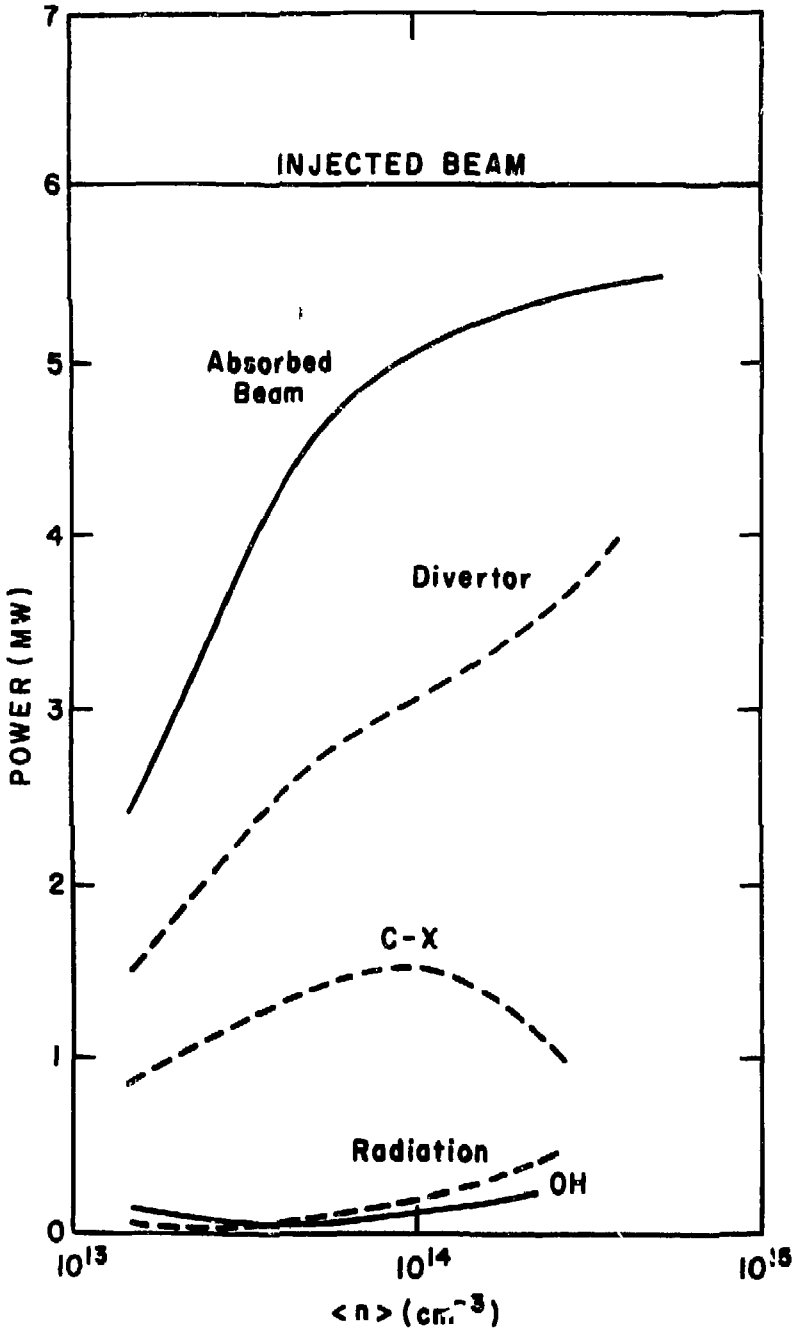

Fig. 9. Power balance vs <n> - PDX w/6 MW beams, 70 eV neutrals.

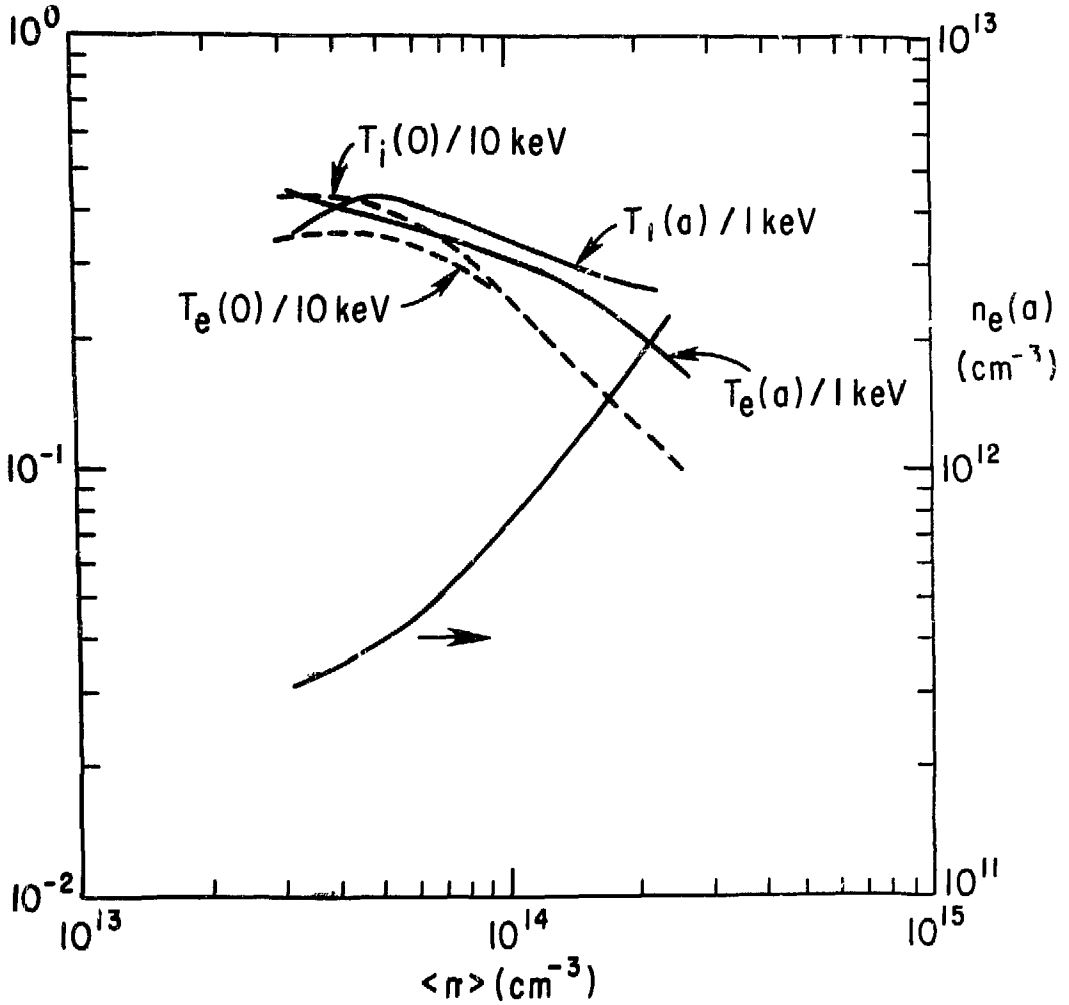

792485

Fig. 10. Edge parameters, central temperatures vs <n> - PDX w/6 MW beams, 300 eV neutrals.

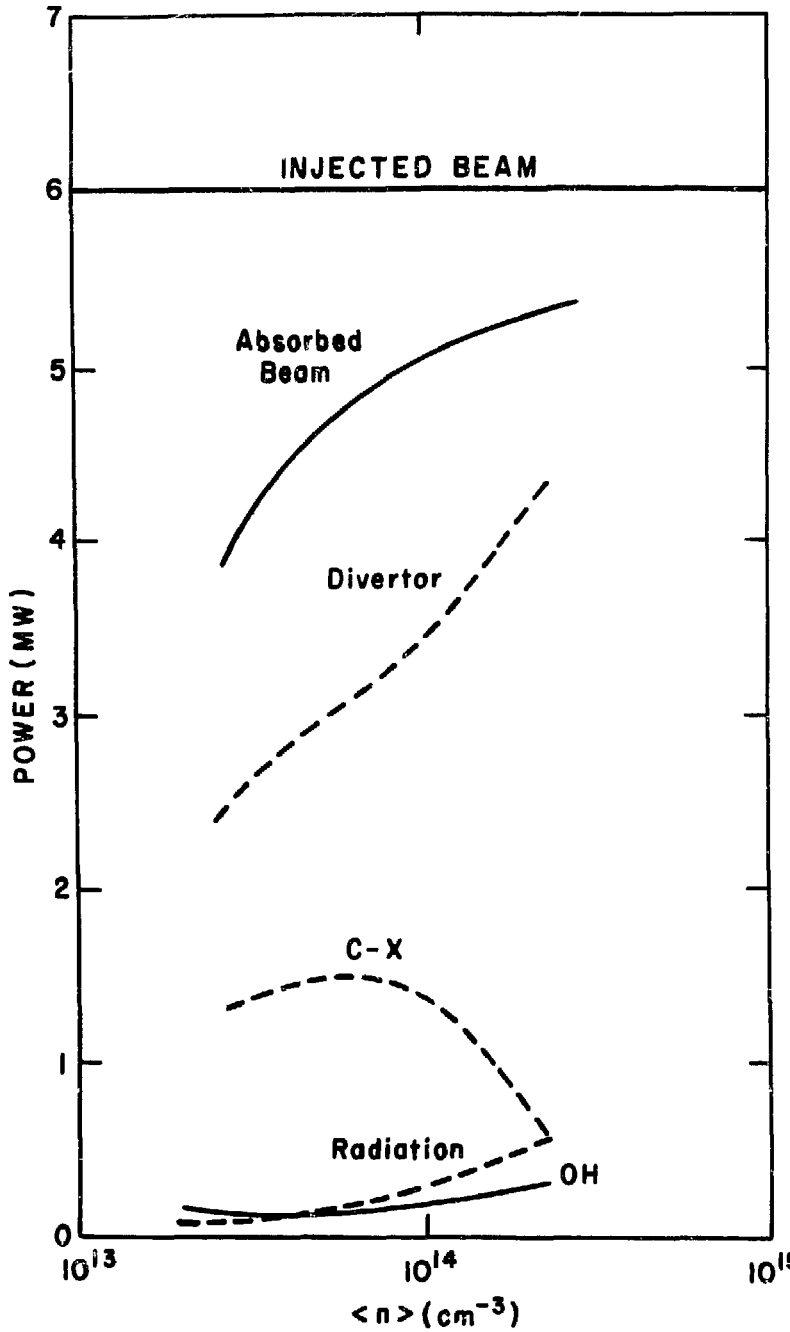

Fig. 11. Power balance vs <n> - PDX w/6 MW beams, 300 eV neutrals.